# Cytokine RNA In Situ Hybridization Permits Individualized Molecular Phenotyping in Biopsies of Psoriasis and Atopic Dermatitis

Alice Wang[1], Alexander L. Fogel[1], Michael J. Murphy[1], Gauri Panse[1,2], Meaghan K. McGeary[2], Jennifer M. McNiff[1,2], Marcus Bosenberg[1,2,3], Matthew D. Vesely[1], Jeffrey M. Cohen[1], Christine J. Ko[1,2], Brett A. King[1] and William Damsky[1,2]

Detection of individual cytokines in routine biopsies from patients with inflammatory skin diseases has the potential to personalize diagnosis and treatment selection, but this approach has been limited by technical feasibility. We evaluate whether a chromogen-based RNA in situ hybridization approach can be used to detect druggable cytokines in psoriasis and atopic dermatitis. A series of psoriasis (n = 20) and atopic dermatitis (n = 26) biopsies were stained using RNA in situ hybridization for *IL4*, *IL12B* (IL-12/23 p40), *IL13*, *IL17A*, *IL17F*, *IL22*, *IL23A* (IL-23 p19), *IL31*, and *TNF* (TNF-α). *NOS2* and *IFNG*, canonical psoriasis biomarkers, were also included. All 20 of the psoriasis cases were positive for *IL17A*, which tended to be the predominant cytokine, although some cases had relatively higher levels of *IL12B*, *IL17F*, or *IL23A*. The majority of cytokine expression in psoriasis was epidermal. A total of 22 of 26 atopic dermatitis cases were positive for *IL13*, also at varying levels; a subset of cases had significant *IL4, IL22, or IL31* expression. Patterns were validated in independent bulk RNA-sequencing and single-cell RNA-sequencing datasets. Overall, RNA in situ hybridization for cytokines appears highly specific with virtually no background staining and may allow for individualized evaluation of treatment-relevant cytokine targets in biopsies from patients with inflammatory skin disorders.

*JID Innovations* (2021);**1**:100021 doi:10.1016/j.xjidi.2021.100021

## INTRODUCTION

Inflammatory dermatologic disorders are increasingly treated with mAbs that inhibit the activity of specific cytokines (biologics). Clinical selection of biologic medicines is done empirically, and it remains unclear why some patients respond to a particular biologic treatment and others do not. For example, in psoriasis, biologics targeting TNF-α, IL-12/23 (p40), IL-17A, IL-17 family (receptor), and IL-23 (p19) are approved. Whereas the majority of patients with psoriasis treated with newer biologics (e.g., IL-17 axis or IL-23 inhibitors) will experience clear or almost clear skin, a subset will not (Bai et al., 2019). In atopic dermatitis (AD), the biologic dupilumab, which targets IL-4Rα and inhibits both IL-4 and IL-13 activity, is approved. However, only approximately one third of patients with AD treated with dupilumab achieve clear or nearly clear skin (Wang et al., 2018). One potential explanation for these observations is that underappreciated immunologic heterogeneity exists across patients, especially across patients with AD, and therefore drugs targeting specific cytokines might be more or less effective for individual patients (Glickman et al., 2020; Tsoi et al., 2019).

Physicians face the increasing challenge of selecting the optimal biologic for individual patients, particularly when many choices might be available for a disease. Apart from medical comorbidities and patient preferences for drug administration, the choice of biologic is generally empirical, and some patients quickly transition to a different agent if they do not experience the desired clinical response. This practice is suboptimal because biologic therapies can have significant adverse effects and are expensive. Ideally, immunologic parameters, including the presence or absence as well as the relative abundance of treatment-relevant cytokines, could be measured in individual patients to help guide personalized diagnosis and treatment. Currently, there are no widely utilized methodologies to assess an individual patient's cytokine profile as part of clinical practice.

Previous attempts to characterize cytokine expression or immune polarization (e.g., type 1 vs. type 2 vs. type 17) in skin biopsies with approaches such as immunohistochemistry (IHC) while innovating in concept have been hampered by high background staining owing to nonspecific binding of antibody, limiting interpretation of true positive staining (Cohen et al., 2020; Miranda et al., 2021; Moy et al., 2015). Immunofluorescence, which can be more specific in some instances, is more technically challenging and typically requires specialized tissue collection and processing. For

[1]Department of Dermatology, Yale School of Medicine, New Haven, Connecticut, USA; [2]Department of Pathology, Yale School of Medicine, New Haven, Connecticut, USA; and [3]Department of Immunobiology, Yale School of Medicine, New Haven, Connecticut, USA

Correspondence: William Damsky, Department of Dermatology, Yale School of Medicine, 333 Cedar Street, LCI 501, PO Box 208059, New Haven, Connecticut 06510, USA. E-mail: william.damsky@yale.edu

Abbreviations: AD, atopic dermatitis; Cat, catalog; DC, dendritic cell; IHC, immunohistochemistry; ILC, innate lymphoid cell; KC, keratinocyte; LC, Langerhans cell; RISH, RNA in situ hybridization; RNA-seq, RNA sequencing; scRNA-seq, single-cell RNA sequencing

Received 14 December 2020; revised 23 March 2021; accepted 30 March 2021; accepted manuscript published online 7 May 2021; corrected proof published online 29 May 2021

Cite this article as: JID Innovations 2021;1:100021

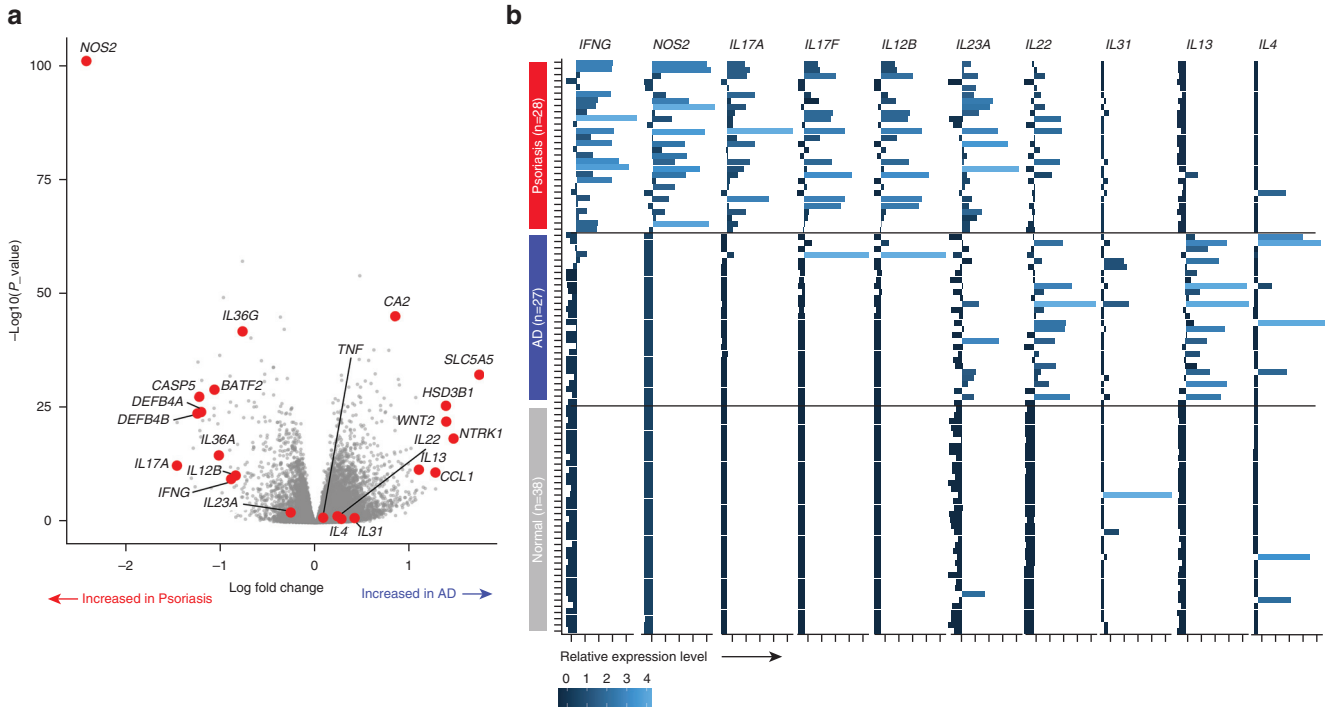


**Figure 1. Cytokine expression patterns differentiate psoriasis and AD, but heterogeneity exists.** (**a**) Volcano plot showing the relative mRNA expression of selected genes in cases of psoriasis (n = 28) and in cases of AD (n = 27) on the basis of analysis of RNA-seq data (Tsoi et al., 2019). (**b**) mRNA expression levels of selected genes among individual patients with each diagnosis, corresponding to data in (**a**). AD, atopic dermatitis; RNA-seq, RNA sequencing.

example, a recent study using carefully selected molecular immunologic makers of type-2 versus those of type-17 inflammation was unable to use the markers to distinguish between cases of psoriasis and AD (Cohen et al., 2020). Although powerful, RNA sequencing (RNA-seq), a widely used research approach to characterize gene expression profiles in tissue, is time consuming and expensive and requires specialized tissue processing, equipment, and expertise, making its incorporation into routine clinical care impractical.

RNA in situ hybridization (RISH) uses nucleic acid–based probes to detect mRNA. A potential advantage of this approach is that the probes are highly specific, and labeling can be visualized in formalin-fixed, paraffin-embedded specimens using chromogenic approaches akin to those used for IHC. Despite its potential utility in this setting, RISH has largely been overlooked in clinical dermatology, including in the area of inflammatory dermatoses.

In this study, we evaluated the ability of RISH to detect pathogenic cytokines in psoriasis and AD and compared the patterns with those in normal skin from healthy controls. We focused on established treatment targets with approved drugs (*IL4*, *IL13*, *IL12B*, *IL17A*, *IL17F*, *IL23A*, *TNF*), emerging therapeutic targets in AD (*IL22*, *IL31*), and canonical psoriasis biomarkers (*NOS2*, *IFNG*) (Garzorz-Stark et al., 2016; He et al., 2021; Quaranta et al., 2014). We assessed the ability of RISH-based cytokine profiles to distinguish between the cases of psoriasis and those of AD as well as to study the intrapatient cytokine heterogeneity within each diagnosis. RISH staining patterns were compared with previously published bulk RNA-seq and single-cell RNA-seq (scRNA-seq) data from psoriasis and AD (Reynolds et al., 2021; Tsoi et al., 2019).

## RESULTS

### Cytokine expression patterns differentiate between psoriasis and AD, but heterogeneity exists

To broadly understand which cytokines and other markers are most different between psoriasis and AD lesions, we analyzed bulk RNA-seq data from lesional skin in a cohort of patients with psoriasis (n = 28), those with AD (n = 27), and healthy controls (n = 38) (Tsoi et al., 2019). We found that *NOS2* (encoding inducible nitric oxide synthase) was markedly upregulated in psoriasis and was the most significantly differentially expressed transcript between the two conditions (Figure 1a). *NOS2* upregulation in psoriasis has been observed previously (He et al., 2021; Quaranta et al., 2014).

We also observed that genes encoding cytokine targets of approved treatments were among the most differentially expressed transcripts. In particular, *IL17A* and *IL13* were markedly upregulated in psoriasis and AD, respectively. *IL12B* (encoding IL-12/23 p40), *IL23A* (encoding IL-23 p19), and *IL17F* were also upregulated in psoriasis, as expected. Significant *IL4* expression was not detected in these samples, although it did tend to be higher in AD, consistent with previous reports (Tsoi et al., 2019). Emerging treatment targets, including *IL31* and *IL22* as well as *IL36A/G*, were increased in AD and psoriasis, respectively.

Next, we assessed the heterogeneity in the expression of key cytokines within these samples. We found that there was considerable variability within both psoriasis and AD in terms of the predominant druggable cytokine expressed

**Table 1. Patient Characteristics**

| Characteristics | Psoriasis | Atopic Dermatitis | Normal |
|---|---|---|---|
| Number of patients | 20 | 26 | 10 |
| Age, y, median (range) | 48 (18–79) | 57 (24–83) | 50 (30–72) |
| Sex, % M; % F | 70 M; 30 F | 68 M; 32 F | 23 M; 77 F |
| Anatomic site, n/total (%) | | | |
| Trunk | 7/20 (35) | 7/26 (27) | 5/10 (50) |
| Extremities | 11/20 (55) | 16/26 (61) | 5/10 (50) |
| Acral | 2/20 (10) | 1/26 (4) | 0/10 (0) |
| Head/neck | 0/20 (0) | 2/26 (8) | 0/10 (0) |

Abbreviations: F, female; M, male.

(Figure 1b). For example, some cases of psoriasis were *IL17A* predominant, but others expressed very little *IL17A* and were instead *IL17F*, *IL23A*, and/or *IL12B* predominant. Interestingly, some cases of AD did not show significant expression of either *IL13* or *IL4*, and one case was *IL17F* predominant. These data suggest that there is significant molecular heterogeneity among cases of psoriasis and AD, which might have important implications for optimal treatment selection.

### Inducible nitric oxide synthase (encoded by *NOS2*) staining differentiates psoriasis from AD

To assess RISH staining in this setting, we assembled cohorts of patients with psoriasis (n = 20) and AD (n = 26) in which biopsy tissue was available for study (Table 1). We first evaluated whether RISH staining for *NOS2* differed between psoriasis and AD, as would be predicted from the analysis of the RNA-seq data. Remarkably, we found that *NOS2* staining was present in all the 20 psoriasis cases and that only 1 of 26 cases of AD had any detectable *NOS2* expression, and this expression was minimal (Figure 2a–c). No staining was observed in any of the normal controls. *NOS2* staining in psoriasis was positive in keratinocytes (KCs) in the upper stratum spinosum (Figure 2b). The apparent specificity of *NOS2* with little background emphasized the potential power of RISH as an approach and also provided molecular immunologic validation of the clinicopathologic classifications for cases included in this series.

### *IL17A* and *IL13* staining patterns also differentiate psoriasis from AD

Analysis of the RNA-seq data suggested that *IL17A* and *IL13* might have the best ability to differentially label psoriasis and AD. Furthermore, IL-17A and IL-13 are key targets of treatment in these disorders. We therefore stained cases using RISH probes specific for *IL17A* and *IL13*. We found that all the 20 cases of psoriasis showed detectable *IL17A* expression in the epidermis (Figure 3a and b). Interestingly, there were significantly fewer *IL17A*-positive cells in the dermis, despite the majority of the inflammation being present in the dermis. As with the RNA-seq data, we found that there was considerable variability in the relative abundance of *IL17A* among psoriasis cases. In contrast, only 2 of the 26 cases of AD had any detectable *IL17A*-positive cells in the epidermis, and staining was minimal. This may support previous literature suggesting that IL-17 may play a driver role in a small subset of patients with AD (Ungar et al., 2021). *IL17A* staining was not observed in any of the normal controls.

*IL13* staining was observed in 85% of the AD cases (Figure 3c and d). Whereas some cases had epidermal predominant *IL13*, other cases had dermal predominant or exclusive expression (Figure 3c and d). The abundance of *IL13*-positive cells was also quite variable in the AD cases. Most cases of psoriasis were negative for *IL13*; however, focal staining was observed in some cases. No *IL13* staining was observed in normal skin. Overall, *IL17A* and *IL13* staining patterns alone were sufficient to distinguish between psoriasis (*IL17A* predominant), AD (*IL13* predominant), and normal (negative staining) in 52 of the 56 cases in the series.

### *IL17A* and *IL13* RISH staining is found predominantly in CD3+ T cells

In both *IL17A* and *IL13* RISH stains, cells that stained positively tended to have a lymphocyte morphology as would be expected. To explore this and also to further validate the specificity of the approach, we performed double staining for CD3 (IHC) and for either *IL17A* or *IL13* in seven randomly selected cases each of psoriasis and AD. We found that the vast majority of *IL17A*- and *IL13*-positive cells also colabeled with CD3, suggesting that they may represent type-17– and type-2–polarized T cells, respectively (Figure 4a and c). We focused on the relative abundance of intraepidermal cytokine-producing T cells as a function of total T cells in the epidermis because particularly in psoriasis, most cytokine-producing cells were found here. This analysis showed that cytokine-producing T cells ranged from 3.5% to 15.1% of all intraepidermal T cells in these samples (Figure 4b and d).

### *IL17F* levels generally correlate with *IL17A* levels in psoriasis

IL-17F is highly homologous to, is often coexpressed with, and can act synergistically with IL-17A (McGeachy et al., 2019). It is conceivable that some cases of psoriasis might be relatively more dependent on IL-17F (or IL-17C) given the observation that some patients respond better to IL-17R blockade than to IL-17A blockade (Kimmel et al., 2019). We next investigated the expression of *IL17F* in this cohort and compared this with *IL17A* expression. We found that *IL17F* was detectable in 19/20 cases of psoriasis and, similarly to *IL17A*, was generally present in the epidermis (Figure 5a and b). As expected, *IL17A* tended to be the predominant cytokine in most cases of psoriasis and was highly correlated with *IL17F*, whereas it was inversely correlated with *IL13* (Figure 5c and d). Interestingly, however, in three cases of psoriasis, *IL17F* was predominant. There was either no or negligible *IL17F* expression in most cases of AD, and no expression was observed in healthy controls.

### *IL4, IL22, IL31, IL12B* (IL-12/23 p40), and *IL23A* (IL-23 p19) staining can also be used to characterize psoriasis and AD

We next used RISH probes for *IL4*, *IL12B*, and *IL23A* to further characterize the skin biopsies from these patients and assess what additional information they might provide, given that there are approved drugs that target these cytokines. We found that *IL4* expression was much lower than that of *IL13* and was not detected at significant levels in the epidermis of most cases of AD (Figure 6a and d). The predominance of *IL13* over *IL4* in AD lesional skin is consistent with previous reports (Bieber, 2020; Tsoi et al., 2019). The expression of *IL4*

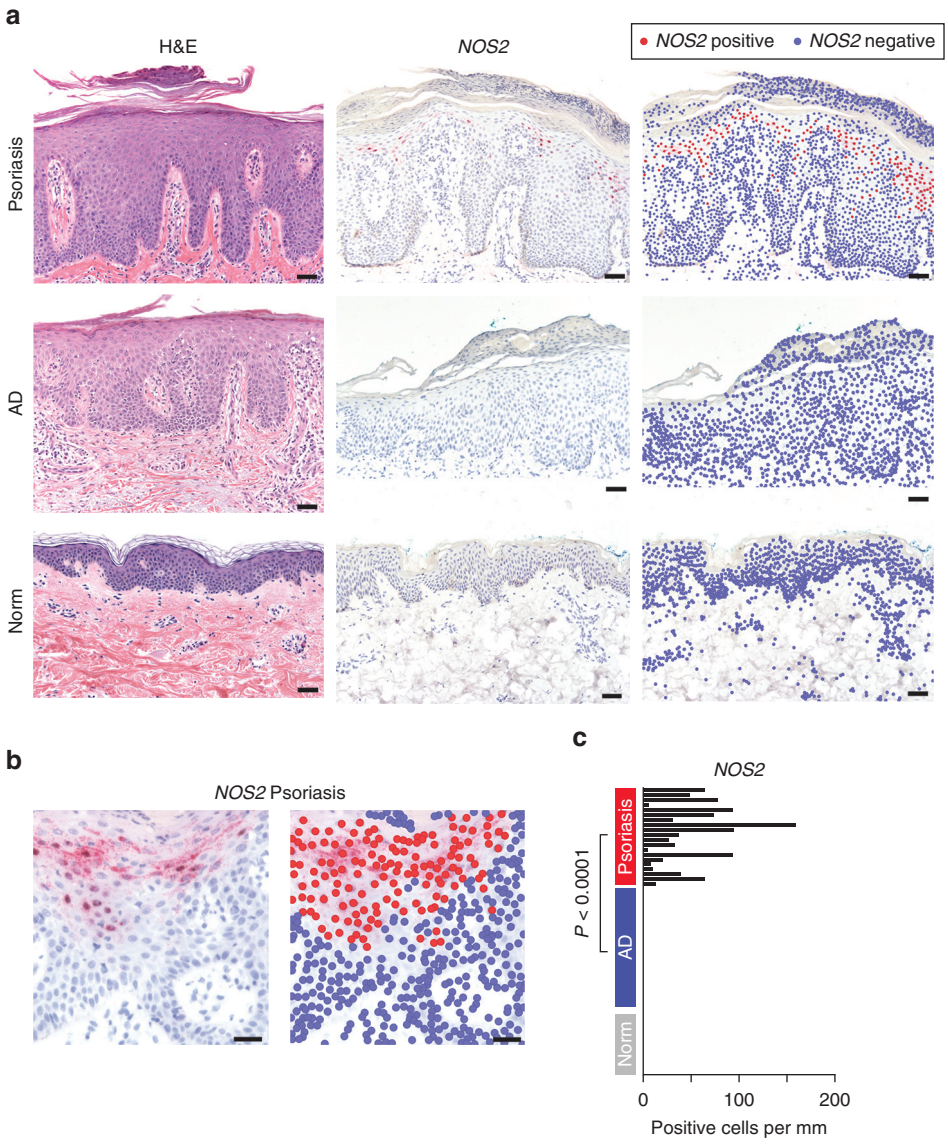


**Figure 2. *NOS2* RISH staining differentiates psoriasis from AD and from normal skin.** (**a**) H&E-stained sections (left panels), *NOS2* RISH staining (middle panels), and quantitative analysis (right panels). Representative cases are shown for each psoriasis case, AD case, and normal controls. Bar = 100 μM. (**b**) *NOS2* RISH staining in a representative case of psoriasis. Bar = 50 μM. (**c**) Quantification of *NOS2* RISH in psoriasis, AD, and normal skin, shown as the number of positive cells per millimeter of the epidermis. AD, atopic dermatitis; Norm, normal; RISH, RNA in situ hybridization.

in some cases but not in others is interesting and might be important in the setting of IL-13–specific inhibition, which is being evaluated in AD.

*IL12B* (IL-12/23 p40) staining within the epidermis was significantly higher in psoriasis than in AD; however, in the dermis, staining was present in both (Figure 6b and d). The significance of *IL12B* staining in the dermis of some of the AD cases is unclear and may represent bystander cells and/or cells producing but not secreting IL-12/23. Of note, we also observed *IL12B* expression in some AD cases in the bulk RNA-seq experiments (Figure 1b). Interestingly, IL-12/23 (p40) expression has been previously reported in AD, especially in chronic cases (Caproni et al., 2007; Yawalkar et al., 2000), and rarely, patients with AD can improve with ustekinumab (Khattri et al., 2017; Shroff and Guttman-Yassky, 2015). No staining for *IL12B* was observed in the normal controls. *IL23A* (IL-23p19) staining within the epidermis was present in most of the psoriasis cases and was rarely present in AD cases (Figure 6c and d). Relatively less staining for *IL23A* was present in the dermis of both conditions. We were struck that most of the detectable *IL23A* production using this approach in psoriasis was in the epidermis, as opposed to that in the dermis. No staining for *IL23A* was observed in the normal controls.

Interestingly, the predominance of staining for both *IL12B* and *IL23A* in psoriasis was within the epidermis. Whereas clusters of positive cells predominated in psoriasis, only individual positive cells were present in positive cases of AD (Figure 7a and b). Although IL-12 and IL-23 have been reported to be predominantly produced by dendritic cells (DCs) in the dermis in psoriasis (Hawkes et al., 2018), production by DCs that either enter the epidermis or reside in the epidermis (e.g., Langerhans cells [LCs]) in psoriasis has also been described (Martini et al., 2017; Nakajima et al., 2019).

We also stained the cases using probes for *IL22*, *IL31*, *IFNG* (IFN-γ), and *TNF* (TNF-α). As expected, *IFNG* staining was increased in psoriasis relative to that in AD (Figure 7c). IL-31 and IL-22 are emerging treatment targets in AD. Although IL-22 inhibition in AD has been overall less effective than hoped, cases with significant IL-22 expression

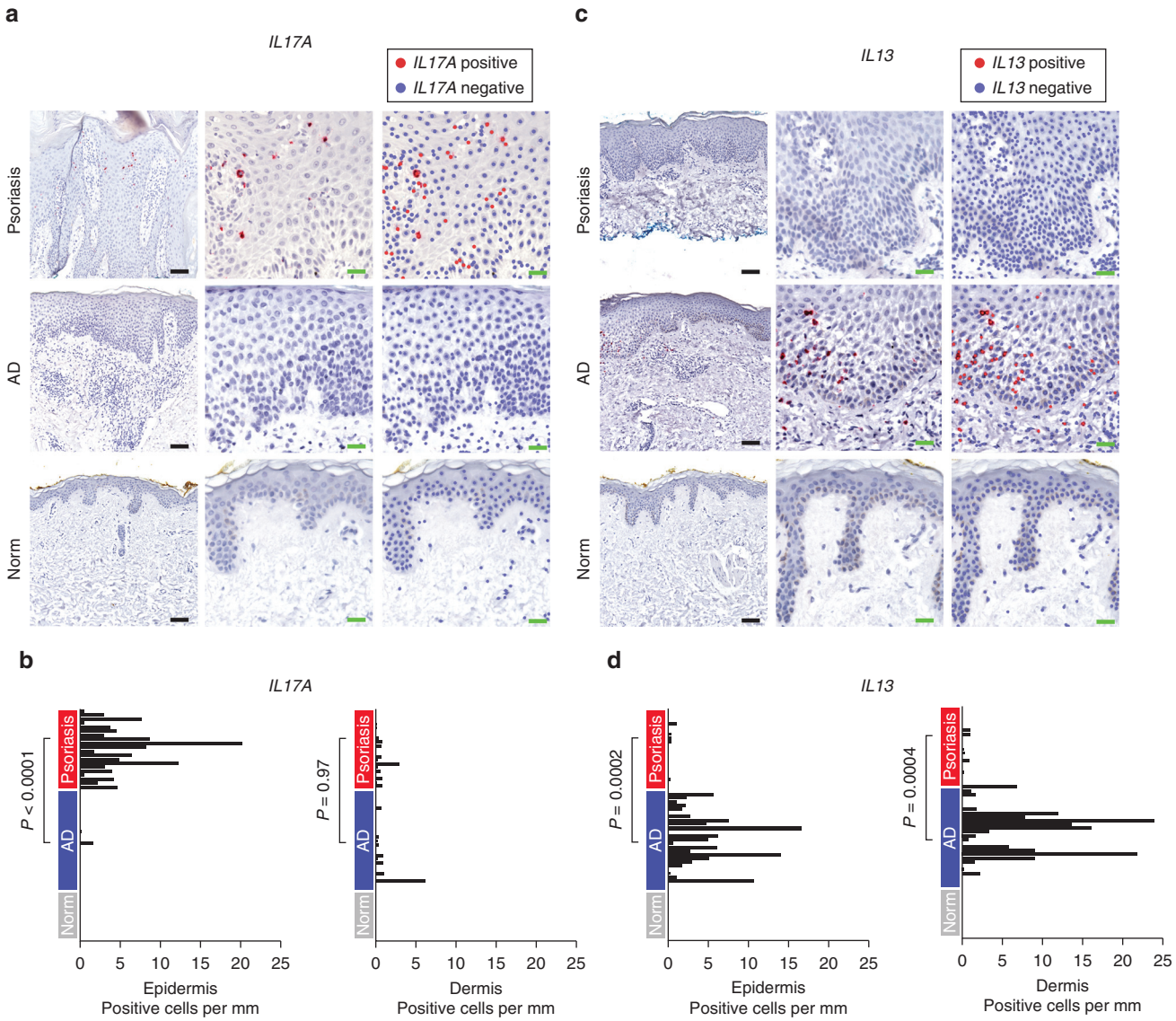


**Figure 3. *IL17A* and *IL13* RISH staining patterns differentiate psoriasis from AD and from normal skin.** (**a**) *IL17A* RISH staining (left and middle panels) and quantitative analysis (right panels). Black bar = 100 μM, green bar = 30 μM. Representative images are shown for each psoriasis, AD, and normal skin. (**b**) Quantification of *IL17A* RISH staining data in psoriasis, AD, and normal controls. The number of positive cells in the epidermis (left) and dermis (right) was quantified independently. (**c**) *IL13* RISH staining (left and middle panels) and quantitative analysis (right panels). Black bar = 100 μM, green bar = 30 μM. Representative images are shown for each psoriasis, AD, and normal controls. (**d**) Quantification of *IL13* RISH staining data in psoriasis, AD, and norm controls; the number of positive cells in the epidermis (left) and dermis (right) was quantified independently. AD, atopic dermatitis; Norm, normal; RISH, RNA in situ hybridization.

appear to respond more optimally to IL-22 blockade (Brunner et al., 2019). IL-22 has also been implicated in psoriasis and may be a cytokine associated with epithelial hyperplasia during chronic inflammation (Zheng et al., 2007). We found that IL-22 was slightly higher in AD cases but was not significantly different between psoriasis and AD (Figure 7c). IL31 was significantly upregulated in AD compared with that in psoriasis; most expression was present in the dermis (Figure 7c).

*TNF* staining was not able to distinguish between AD and psoriasis (Figure 7c). Analysis of bulk RNA-seq data (Figure 1a) also showed this. This has been described previously and may relate to the observation that *TNF* mRNA is preproduced intracellularly and held under translational repression (Salerno et al., 2018), and so measurement of mRNA levels may not accurately estimate TNF-α activity.

### Analysis of cytokine expression patterns with scRNA-seq

Overall, with the RISH staining, we were struck by the epidermal predominant expression of type-17 cytokines, including *IL17A*, *IL17F*, *IL12B*, and *IL23A*, in psoriasis. To further evaluate this finding, we turned to a recently published scRNA-seq study of psoriasis and AD by Reynolds et al. (2021). In this study, the authors used scRNA-seq to compare between psoriasis (n = 3), AD (n = 4), and healthy skin (n = 5). Before dissociation for scRNA-seq, the epidermis and dermis were separated from each other and were analyzed in distinct samples for each case. Thus, this provided an ideal dataset with which to validate epidermal

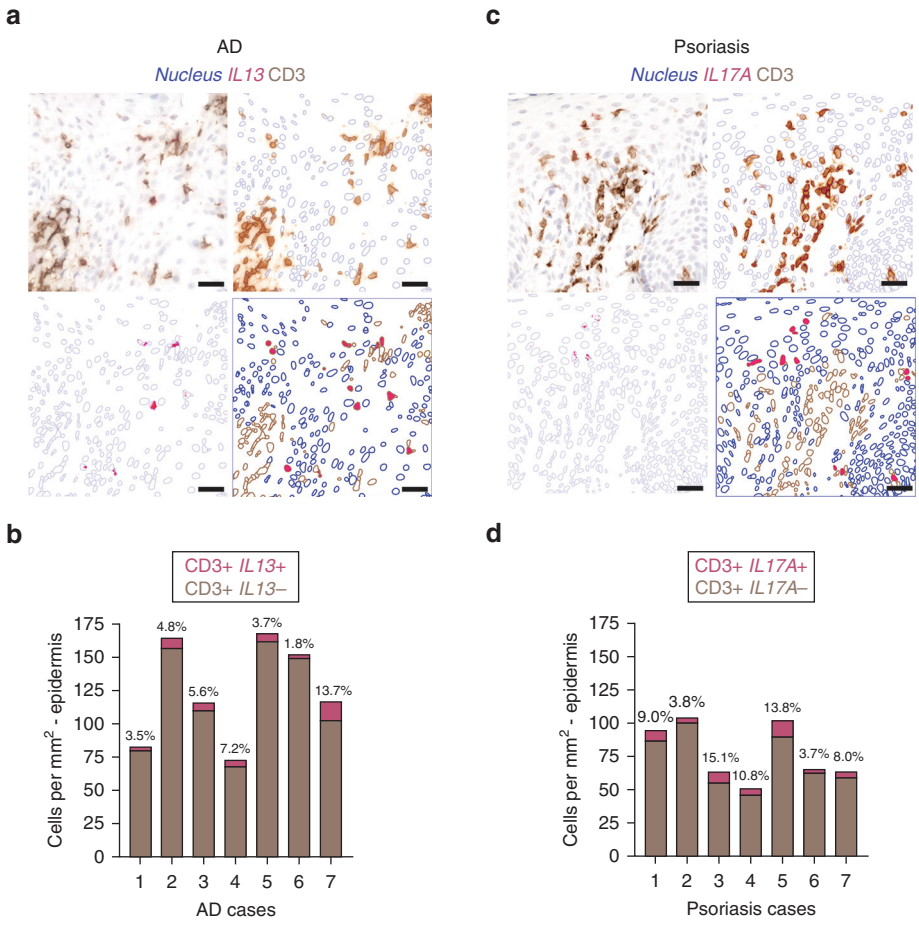


**Figure 4. *IL13* and *IL17A* expressions localize to CD3+ T lymphocytes.** (**a**) Double stain showing *IL13* RISH (red) and CD3 IHC (brown) in a representative case of AD. Bar = 30 μM. Representative analysis using QuPath and ImageJ is shown. (**b**) Quantification of the number of *IL13*-positive cells as a function of total CD3+ cells in AD epidermis (n = 7). (**c**) Double stain showing *IL17A* ISH (red) and CD3 IHC (brown) in a representative case of psoriasis. Bar = 30 μM. Representative analysis using QuPath and ImageJ is shown. (**d**) Quantification of the number of *IL17A*-positive cells as a function of the total CD3+ cells in psoriasis epidermis (n = 7). AD, atopic dermatitis; IHC, immunohistochemistry; ISH, in situ hybridization.

versus dermal cytokine mRNA expression patterns as determined by RISH as well as cell-type specificity of expression.

There were 528,253 cells in the study by Reynolds et al. (2021). We focused only on T cells, innate lymphoid cells (ILCs), NK cells, other myeloid cells, and KCs according to the cell-type designations as determined by the original authors. In addition, we only analyzed data from lesional skin samples, resulting in a total of 127,219 cells for analysis. Clustering of these data was visualized using t-distributed Stochastic Neighbor Embedding (Figure 8a, b, and d). Next, we looked at the proportion of T cells in the epidermal versus the proportion in the dermal preparations across the samples. In psoriasis, although most T cells were located in the dermis, the vast majority of *IL17A*-producing T cells were found in the epidermis (Figure 8c). In contrast, although T cells were more evenly distributed between the epidermis and the dermis in AD, the majority of *IL13* production was in the dermis (although there was some in the epidermis too) (Figure 8c). Overall, these patterns are highly consistent with our RISH data, although we did detect relatively more epidermal *IL13* in our samples.

Next, we looked more broadly at cytokine expression among T cells, NK cells, ILCs, macrophages, DCs, and KCs as a function of epidermal versus that of dermal derivation (Figure 8e). Most cytokine expression was from T cells, consistent with our observations, but some were also found in ILCs and NK cells. In psoriasis, the majority of *IL12B* and *IL23A* expression was from myeloid cells (Figure 8f). DCs in the epidermis produced the highest levels of *IL12B* in psoriasis. Whereas the magnitude of *IL23A* expression was higher in the epidermis, the proportion of cells producing *IL23A* was slightly higher in the dermis.

### Principal component analysis using RISH patterns distinguishes psoriasis from AD

Finally, we performed principal component analysis on these cases using the cytokine and *NOS2* RISH staining data. This analysis showed that psoriasis cases generally clustered together and that AD cases also generally clustered together (Figure 9a–c). Biplot analysis of the principal component analysis plots showed that *IL13, IL4, IL31,* and *IL22* were the drivers of clustering along the AD principal component PC2, whereas *NOS2, IL17A, IL17F, IFNG, IL23A,* and *IL12B* were the drivers of clustering along the psoriasis principal component PC1.

## DISCUSSION

In the past several years, there has been a revolution in the molecularly directed treatment of inflammatory skin diseases, including psoriasis and AD. However, clinically implementable and actionable molecular diagnostics in this area have lagged, particularly as they might relate to personalized treatment selection. A trial-and-error approach to biologic

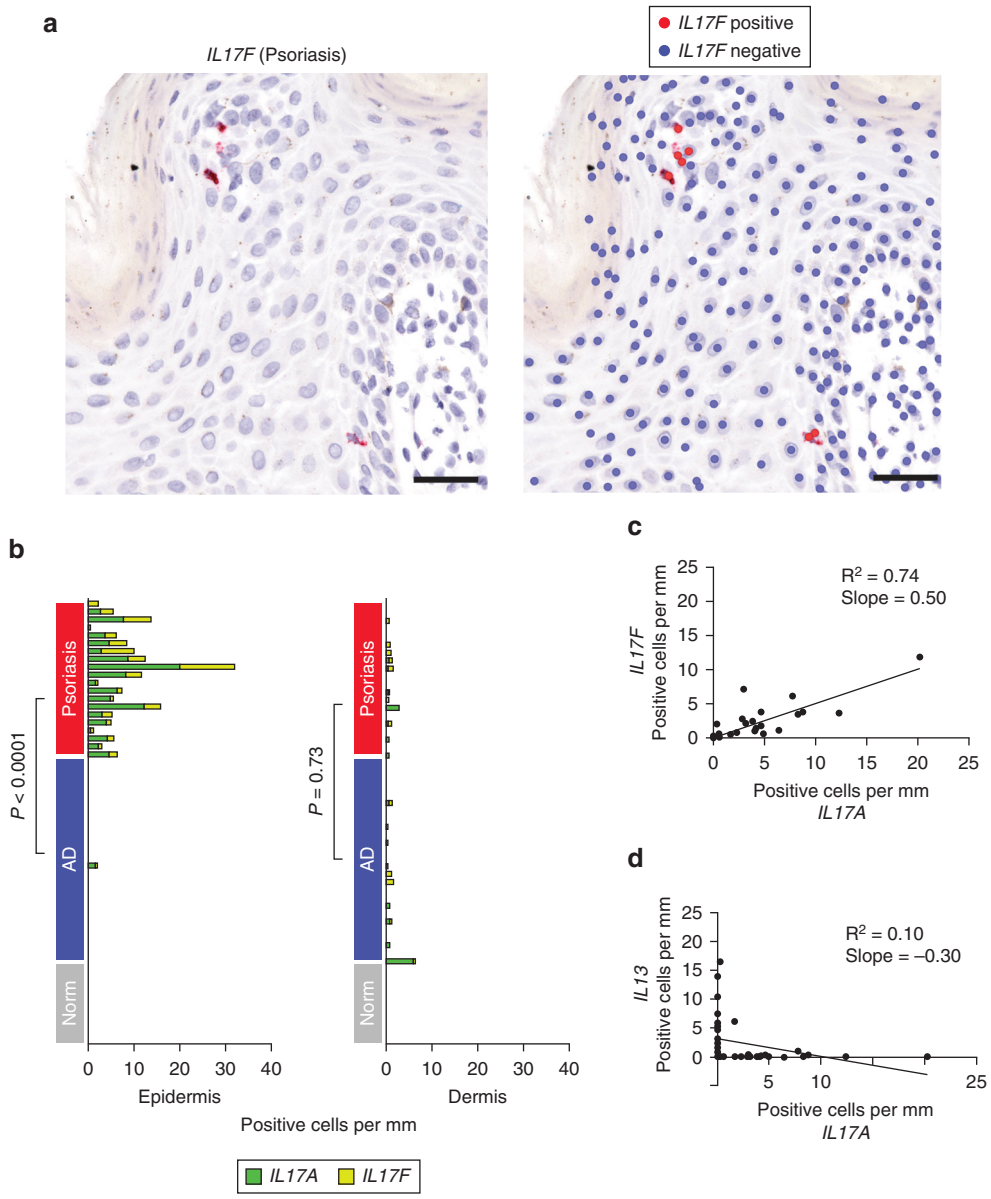


**Figure 5. *IL17F* staining correlates with *IL17A* staining in psoriasis.** (**a**) *IL17F* RISH staining (left panel) and quantitative analysis (right panel) in a representative case of psoriasis. Bar = 100 μM. (**b**) Quantification of *IL17A* and *IL17F* RISH staining. The number of positive cells in the epidermis (left) and dermis (right) were quantified independently. (**c**) Scatter plot of *IL17A* versus that of *IL17F* levels in the epidermis of psoriasis and AD cases. (**d**) Scatter plot of *IL17A* versus that of *IL13* levels in the epidermis of psoriasis and AD cases. AD, atopic dermatitis; Norm, normal; RISH, RNA in situ hybridization.

treatment remains standard of care; however, such an approach (i) is inefficient, (ii) is expensive, (iii) is potentially anxiety inducing to patients because treatment outcomes are unpredictable, and (iv) may be accompanied by potentially avoidable adverse effects. In addition, some patients may remain on a medication to which they have a suboptimal response when a better alternative in a different class may be available (e.g., IL-12/23p40 vs. IL-17A vs. IL-23 inhibitor in psoriasis).

In this study, we show that RISH for disease-causing cytokines is a specific, feasible approach that can identify pathologic cytokines in psoriasis and AD, with *IL17A* and *IL13* appearing to provide the most information. RISH is also an approach that can be easily and cost-efficiently implemented in dermatopathology laboratories because its workflow is analogous to that of IHC. The results are also rapid, making it conceivable that data obtained through RISH-based analyses could be incorporated into real-time clinical decision making. In contrast, RNA-seq is expensive, requires specialized tissue collection and processing (including data normalization), and can take weeks or more.

We observed that there is variability within both psoriasis and AD in terms of the predominant druggable cytokine expressed. In psoriasis, most cases were *IL17A* predominant, but others were instead *IL17F*, *IL23A*, and/or *IL12B* predominant. Psoriasis cases demonstrated relatively less molecular immunologic heterogeneity than AD cases, consistent with previous observations and with the excellent responses observed with IL-17 and IL-23 inhibitors in most patients with psoriasis. How this molecular heterogeneity relates to differences in response to treatment and potentially to the development of paradoxical eruptions when a particular cytokine is inhibited will be an area of significant interest moving forward.

Interestingly, most *IL17* mRNA expression appeared to be within the epidermis in psoriasis, a pattern observed both in the RISH staining and in the scRNA-seq data. These findings were somewhat surprising because they are not necessarily in

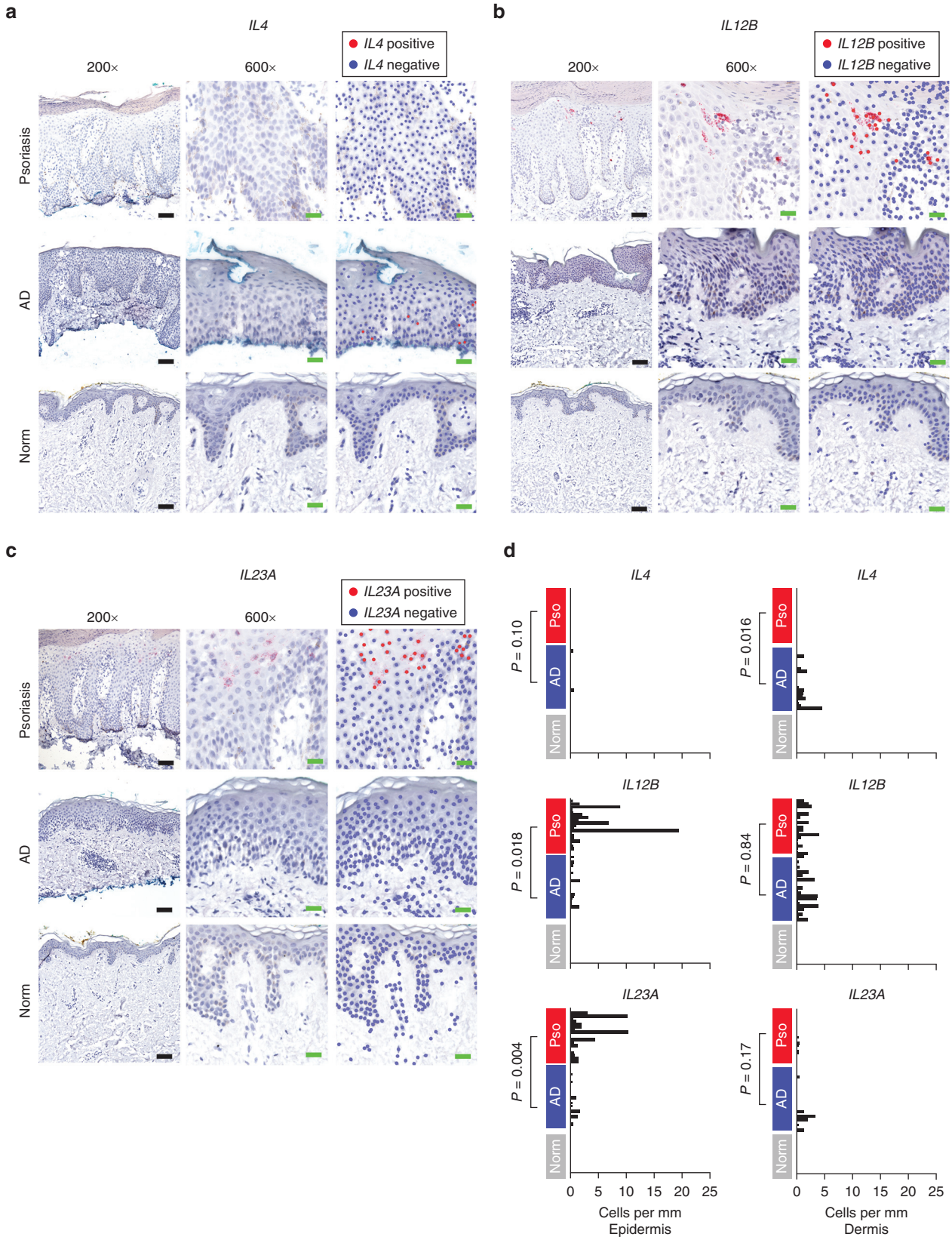


**Figure 6. *IL4, IL12B, and IL23A* staining can also be used to classify cases of psoriasis and AD.** (**a**) *IL4* RISH staining (left and middle panels) and quantitative analysis (right panels). Black bar = 100 μM, green bar = 30 μM. Representative images are shown for each psoriasis, AD, and normal control. (**b**) *IL12B* RISH staining (left and middle panels) and quantitative analysis (right panels). Black bar = 100 μM, green bar = 30 μM. Representative images are shown for each psoriasis, AD, and normal control. (**c**) *IL23A* RISH staining (left and middle panels) and quantitative analysis (right panels). Black bar = 100 μM, green bar = 30 μM. Representative images are shown for each psoriasis, AD, and normal control. (**d**) Quantification of *IL4*, *IL12B*, and *IL23A* RISH in psoriasis, AD, and normal skin shown as the number of positive cells per millimeter of the epidermis (left panels) or dermis (right panels). AD, atopic dermatitis; Norm, normal; Pso, psoriasis; RISH, RNA in situ hybridization.

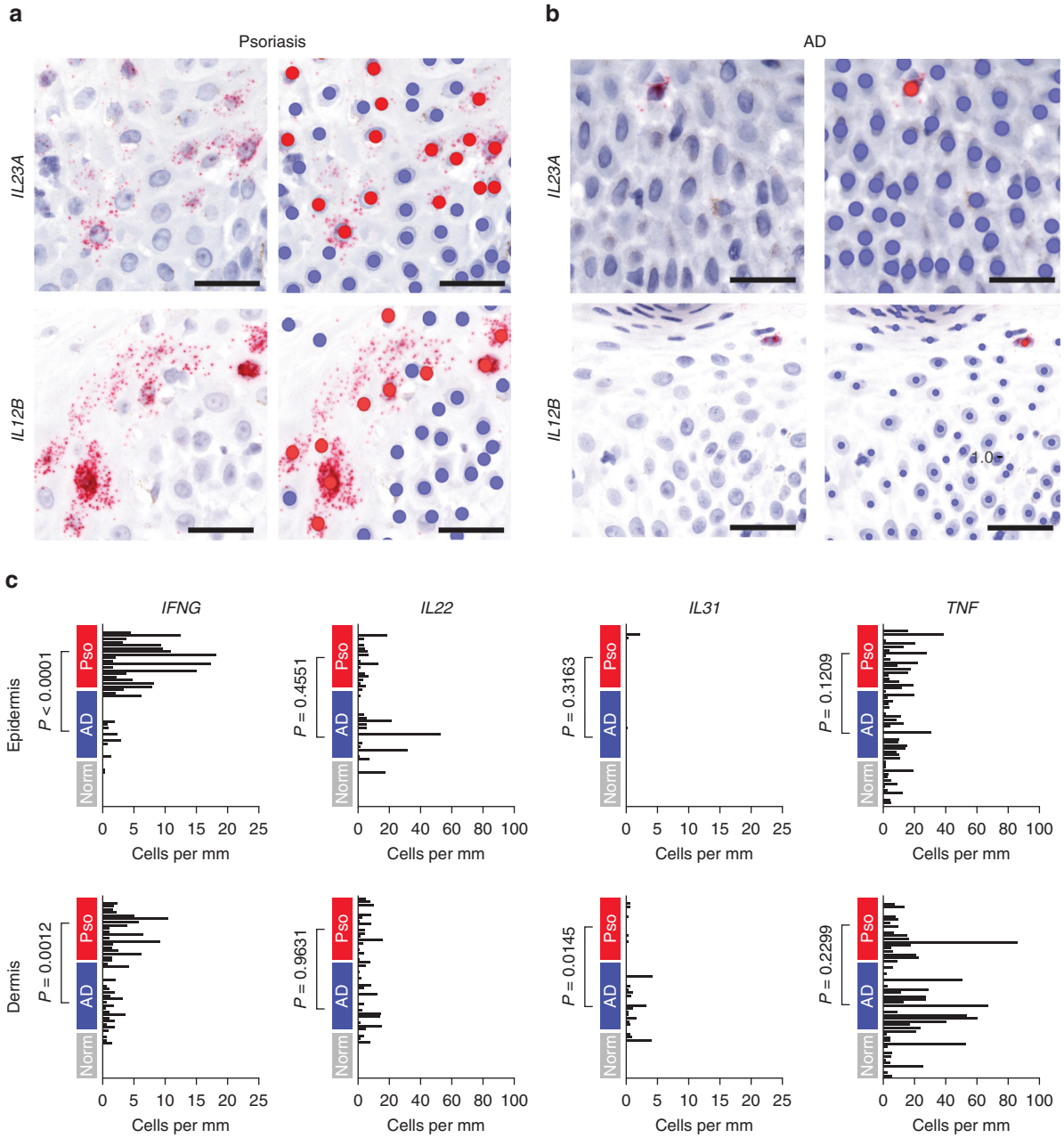


**Figure 7. *IL22, IL31, IFNG,* and *TNF* staining patterns in psoriasis and AD.** (**a**) Representative *IL23A* and *IL12B* staining patterns in psoriasis. Bar = 50 μM. (**b**) Representative *IL23A* and *IL12B* staining patterns in AD. Bar = 50 μM. (**c**) Quantification of *IFNG, IL22, IL31,* and *TNF* RISH in psoriasis, AD, and normal skin, shown as the number of positive cells per millimeter of the epidermis (upper panels) or dermis (lower panels). AD, atopic dermatitis; Norm, normal; Pso, psoriasis; RISH, RNA in situ hybridization.

agreement with previous studies looking at cytokine expression patterns in psoriasis in tissue sections, which have reported mostly a dermal expression of these cytokines using IHC and/or immunofluorescence (Johansen et al., 2010; Miyagaki et al., 2011; Zhang et al., 2010). Additional study will be needed to reconcile these observations, which may relate to differences in technique and detection of mRNA versus of protein.

We also somewhat surprisingly found that most of the *IL12B* and *IL23A* production in psoriasis, as detected by RISH, was within the epidermis compared with that in the dermis. In the scRNA-seq dataset, *IL12B* expression was predominantly epidermal, whereas *IL23A* was produced in both the epidermis and dermis (Reynolds et al., 2021). Previous studies have also found the expression of these cytokines by DCs that either enter the epidermis or reside in the epidermis (e.g., LCs) (Martini et al., 2017; Nakajima et al., 2019), whereas other studies have found mostly dermal expression. There was a negligible expression by KCs. As with IL-17, additional study will be needed to reconcile the differences in location of cytokine production observed in different studies with different techniques.

In AD, although most cases were *IL13* predominant, some cases of AD did not show significant expression of either *IL13* or *IL4,* and one case was *IL17F* predominant. Furthermore, there was relatively more or less *IL22* and *IL31* staining in

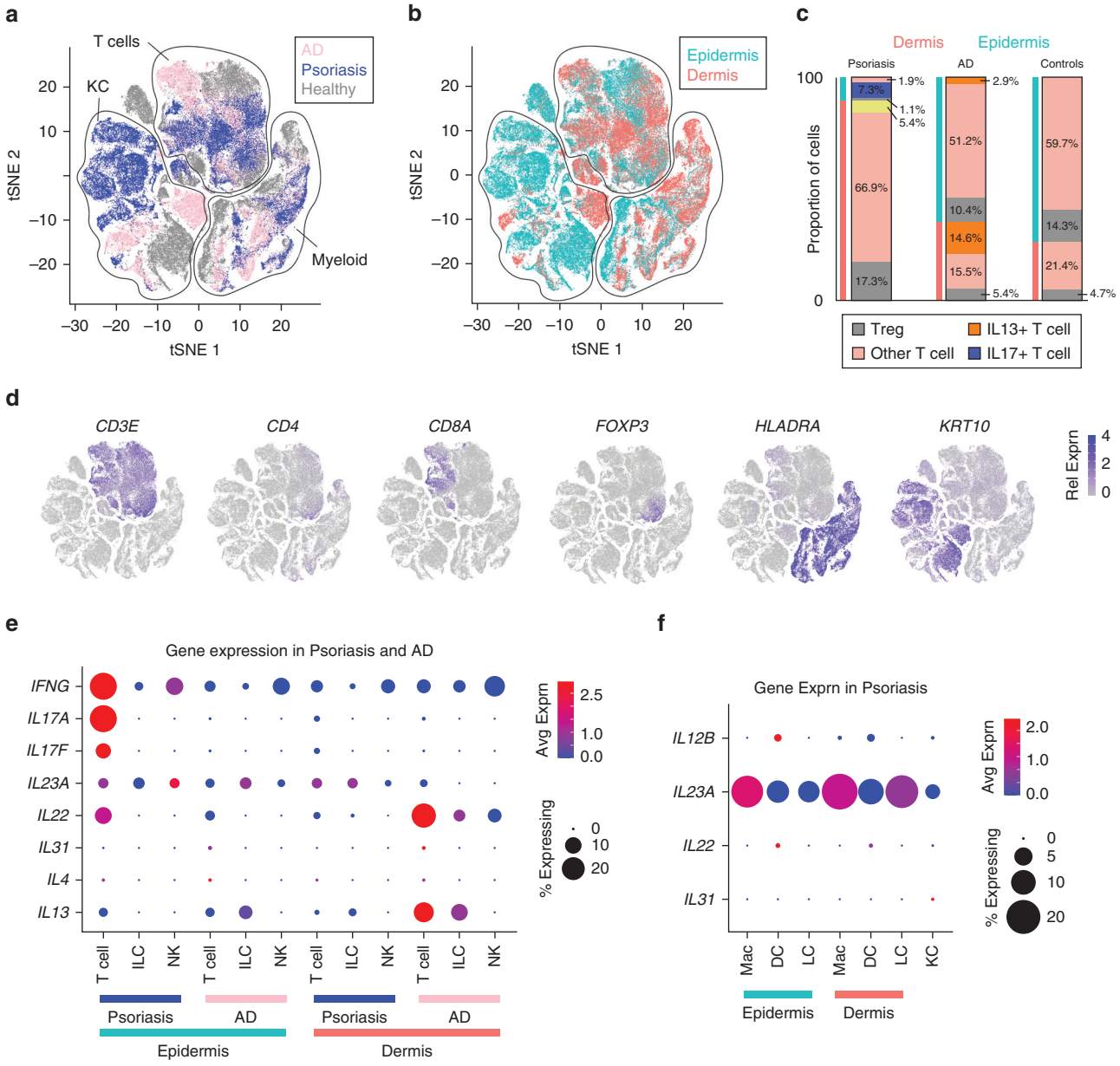


**Figure 8. Analysis of scRNA-seq data in psoriasis (n = 3), AD (n = 4), and normal control (n = 5) skin.** Reanalysis of data from Reynolds et al. (2021). (**a**) t-SNE plot of KCs, myeloid cells, and T cells colored by sample type. (**b**) t-SNE in (**a**) colored by epidermal location versus dermal location. (**c**) Bar graphs showing the proportion of different T cell populations in the epidermis and dermis by diagnosis. (**d**) t-SNE plots from a showing expression patterns of individual genes. (**e, f**) Dot plots showing cytokine expression by various cell types. For **c**–**f**, cell identity is based on designations assigned by Reynolds et al. (2021). AD, atopic dermatitis; Avg, average; Exprn, expression; ILC, innate lymphoid cells; KC, keratinocytes; Mac, macrophages; Rel, relative; scRNA-seq, single-cell RNA sequencing; t-SNE, t-distributed stochastic neighbor embedding.

individual cases. Of note, in occasional cases, *IL13* was not detected at all; whether this represents biology or instead a technical or sampling limitation remains to be determined.

Considerable clinical heterogeneity exists in AD and this may be driven, in part, by underlying immunologic heterogeneity (Czarnowicki et al., 2019; Tsoi et al., 2019). Along these lines, some groups have even divided AD into immunologic endotypes, given the observation that IL-17 may play a more prominent role in children with AD and in patients with AD who are of Asian descent and that IL-22 may play a more prominent role in some African Americans with AD (Czarnowicki et al., 2019). Overall, RISH may provide a practical means by which to dissect this molecular heterogeneity in a quantifiable and practical fashion. We hypothesize that patients with purer *IL13–IL4* dysregulation may respond best to the blockade of this axis with dupilumab, whereas those with mixed or other immunologic drivers may respond suboptimally and may theoretically respond better to blockade of other cytokines or to more broadly acting cytokine blockers, such as Jak inhibitors. Future studies will be required to test this hypothesis.

Limitations of this study include a relatively small sample size, a retrospective design, and the inability to correlate RISH cytokine profiles with treatment response to biologics. In the future, it would also be useful to see how well RISH patterns from different lesions in individual patients correlate

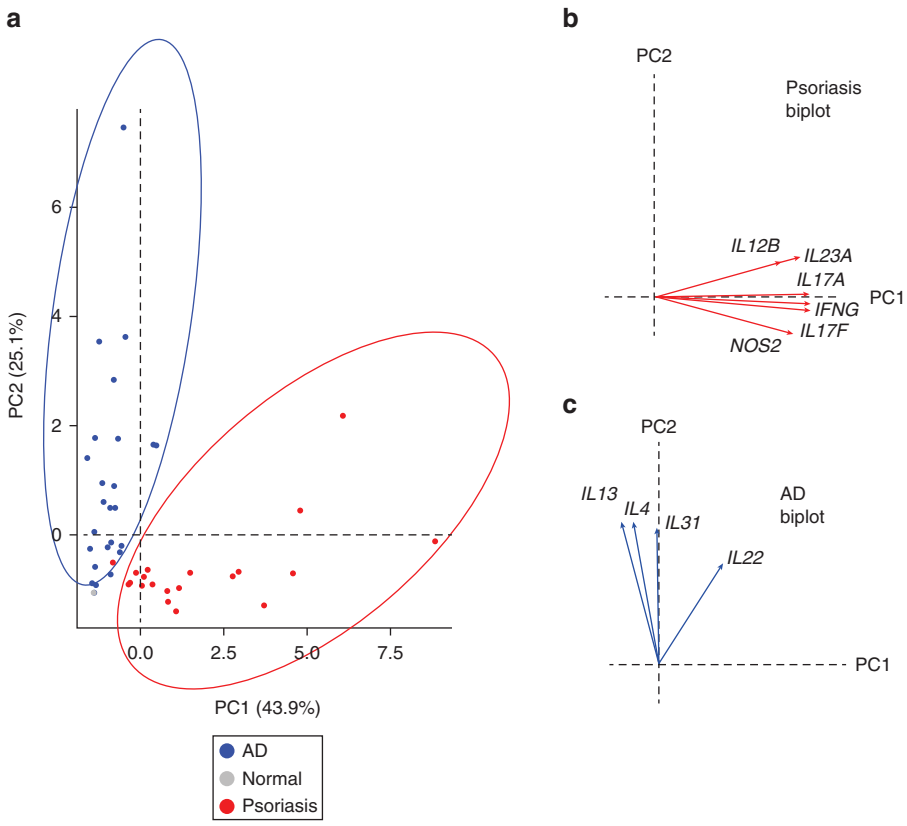


**Figure 9. Psoriasis and AD cases can be classified on the basis of cytokine expression patterns determined by RISH.** (**a**) PCA of psoriasis, AD, and normal controls based on RISH staining pattern for *IL17A*, *IL17F*, *IL12B*, *IL23A*, *NOS2*, *IL13*, and *IL4* in the epidermis. (**b**) Biplot of the PCA data for psoriasis drivers. (**c**) Biplot of the PCA data for AD drivers. AD, atopic dermatitis; PCA, principal component analysis; RISH, RNA in situ hybridization.

with each other in space and time. The patients with AD in the RISH cohort were also older, in general, and may not be fully representative of all patients with AD. Prospective studies of patients starting biologic therapies are needed. The cost of the assay is also a consideration. The cost of each RISH stain is roughly comparable with that of an IHC stain, and so it is unlikely to be practical to perform large cytokine panels on individual cases in clinical practice; however, one might envision scenarios where smaller, more targeted panels could be useful.

This study shows the feasibility of RISH for the detection of cytokines in inflammatory skin diseases. RISH for cytokines could be readily expanded to additional cytokine targets and could be further applied to these and other inflammatory skin diseases. Minimal background staining is observed with the approach, making it very straightforward to quantify and suggesting that reproducibility among different laboratories is likely to be high. Overall, we predict that this approach will be a useful and efficient tool to molecularly phenotype inflammatory skin diseases with implications for both research and clinical care, including personalized treatment selection.

## MATERIALS AND METHODS

### Retrospective case series

Cases were selected after searching the Yale Dermatopathology (New Haven, CT) database for archival material. A total of 20 cases of psoriasis, 26 cases of AD, and 10 cases of normal skin from healthy controls were selected. For psoriasis and AD, biopsies were of lesional skin. For psoriasis, cases were only included if they had classic clinical and histologic features, as determined by board-certified and experienced dermatologists and dermatopathologists. Medical chart review, including a review of clinical photographs to confirm the clinical diagnosis, was performed as needed. AD cases showed typical features of subacute-to-chronic spongiotic dermatitis histopathologically, and the clinical presentation was typical of AD. The clinical diagnosis of AD was made by experienced dermatologists. The clinical presentation was further verified using medical record and clinical photograph review. The Hanifin–Rajka criteria were utilized (Hanifin and Rajka, 1980). Only cases that could be confidently classified as AD on the basis of these criteria were included. The vast majority of biopsies were from adults reflecting biopsy acquisition patterns in AD at our institution. Normal skin from excision tips of nonchronically sun-exposed sites was included as controls. This work was reviewed and approved by the Yale Institutional Review Board.

### RISH

RISH was performed using the RNA scope kit (Bio-Techne, Minneapolis, MN) following the manufacturer's instructions. Briefly, slides were deparaffinized and then treated with hydrogen peroxide and protease from the RNA scope kit (catalog [Cat] #322330). Antigen retrieval was performed with RNA scope target retrieval reagent (Cat #322000). Probe hybridization and amplification steps were then performed according to the manufacturer's instructions. Slides were counterstained with hematoxylin and coverslipped. Probes for *IL17A* (Cat #310931), *IL17F* (Cat #310941), *IL12B* (IL-12 p40) (Cat #402071), *IL23A* (IL-23 p19) (Cat #562851), *IL4* (Cat #315191), *IL13* (Cat #586241), *IL22* (Cat #560811), *IL31* (Cat #436751), *TNF* (TNF-α) (cat # 310421), *IFNG* (310501), and *NOS2* (Cat #424991) were purchased from Bio-Techne. Staining with a positive control probe, for *PPIB* (Cat# 313901), a housekeeping gene (Nazet et al., 2019; Pachot et al., 2004), was performed on five cases each of psoriasis,

AD, and normal skin to ensure equal staining of cells in epidermis and dermis (data not shown). Staining with a negative control probe, *DapB* (Cat #310043), an *E. coli* gene, was performed in a subset of cases and showed no staining (data not shown).

The CD3 IHC was performed using an anti-CD3ε antibody (D7A6E) acquired from Cell Signaling Technology (Danvers, MA) (Cat #85061). Double staining was performed using the RNA scope kit (Bio-Techne) as described earlier, followed by IHC using standard methods. Briefly, after in situ hybridization signal detection, antigen retrieval was performed with citrate buffer (pH 6.0) (Cat #00500, Thermo Fisher Scientific, Waltham, MA). Peroxidase activity was quenched using 3% hydrogen peroxide (Cat# JT-2186-01, JT Baker, Phillipsburg, NJ). The primary antibody was incubated and then detected using a species-specific secondary antibody and the ImmPRESS horseradish peroxidase reagent (Vector Laboratories, Burlingame, CA) and diaminobenzidine substrate (Vector Laboratories). Slides were counterstained with hematoxylin and were coverslipped.

### Quantification of RISH and IHC staining

Slides were scanned using a Hamamatsu Nano Zoomer S210 (Yale Dermatopathology). For certain analyses, QuPath (version 0.2.3) (Bankhead et al., 2017) and ImageJ (Fiji version 2.10) were utilized to assist with quantification (Doube et al., 2010). The number of positive cells in each specimen was quantified separately for the epidermal and dermal portions. The number of positive cells was divided by the width of the biopsy in millimeters to correct for differences in biopsy size (cells per mm). For a cell to be counted as positive, staining needed to be clearly apparent with the ×20 objective, and at least two dots per cell had to be present (most positive cells had >2 dots). Faint single dots apparent only with the ×40 objective were not counted as positive. The slides were scored in a blinded fashion by consensus (AW and WD). Although the diagnosis was not considered during the scoring, morphologic features in some cases could not be entirely ignored.

For singly stained slides, the images were imported into QuPath. A region of interest that covered the area of interest was selected. Stain vectors were defined by selecting a region of interest that was representative of the stain. The positive cell detection feature was utilized to identify the positive cells for each marker. The automated detection was manually verified, and in some cases, adjustments were made manually. To facilitate visualization, cells were colored on the basis of whether or not they were positive for the marker.

For double-stained slides, the images were imported into QuPath, and the color vectors were defined using the region of interest as described earlier. The he_heavy_augement model, a brightfield image nucleus StarDist (arXiv: 1806.03535) approach, was then used in QuPath to detect cell nuclei. After nucleus detection using this approach, the images were then imported into Fiji for color deconvolution on the basis of the stain vectors defined in QuPath. Color deconvolution allowed the separation of the different channels from each stain. Brightness and contrast for each channel were then adjusted (these were done manually) to maximize signal to background ratio using Fiji. The deconvoluted, optimized images were then reoverlaid using Photoshop (version 21.2.0).

### RNA-seq analysis

A previously published, bulk RNA-seq dataset was utilized (Tsoi et al., 2019). Read counts were downloaded from Gene Expression Omnibus (GSE121212). Data analysis was performed using Partek Flow software (version 9.0, build 9.0.20.0510) (Partek, Inc, St. Louis, MI). AD and psoriasis lesional skin and healthy control samples were extracted from the rest of the data set (which also included nonlesional skin). Read counts for these samples were extracted to generate bar graphs using tidyr (version 1.1.0), ggplot2 (version 3.3.2), and data.table (version 1.12.8). The entire dataset was normalized in Partek Flow. DESeq2 was used for differential gene expression analysis to compare psoriasis samples with AD samples in the dataset. The Volcano plot was generated using dplyr (version 1.0.0), ggplot2 (version 3.3.2), and ggrepel (version 0.8.2). The principal component analysis plot was generated by Factoextra (1.0.7) and FactoMineR (2.3) for the manually quantified results.

### scRNA-seq analysis

A recently published scRNA-seq dataset comprising AD, psoriasis, and healthy control skin samples (Reynolds et al., 2021) was analyzed to examine the patterns of cytokine expression. In this study, the epidermal and dermal portions of the tissue were separated and then dissociated and analyzed separately. The data from this study are freely available, and we downloaded them from https://zenodo.org/record/4569496#.YE9kGLRKi-V. We focused our analysis of these data on lesional AD, lesional psoriasis, and healthy control libraries, which were reanalyzed in Seurat (version 3.2.0). Nonlesional AD and psoriasis skin libraries were not included in our analyses. T cells, myeloid cells, and KCs were subsetted on the basis of the cell-type assignments from the original publication, as determined by AutoGeneS, and were then reanalyzed. We retained these cell-type identities for the subsetting because certain analyses groups were combined, for example, T cells (Tc, Tc17_T helper type 17, Tc_IL13_IL22, T helper, regulatory T cell), ILCs (ILC1_NK, ILC2, ILC3), macrophages (Inf_Mac, Macro_1, Macro_2, Mono_Mac), DCs (DC1, DC2, MigDC, moDC_1, moDC_2, moDC_3), LC (LC_1, LC_2, LC_3, LC_4), and KCs (differentiated, proliferating KC, undifferentiated KC). In total, we included 127,219 cells in our analysis of the data. The NormalizeData command with a scale factor of 10,000 was used to normalize counts. The data were then further scaled on the basis of the number of transcripts and center gene expression values. Cells were clustered using FindNeighbors and FindClusters commands. The data were visualized by performing t-Distributed Stochastic Neighbor Embedding. The FeaturePlot command was used to generate gene-specific t-Distributed Stochastic Neighbor Embedding plots, and DotPlot command was used to generate dot plots.

### Statistical analyses

Statistical analyses were performed using GraphPad Prism (version 9.0.0) (GraphPad, San Diego, CA). *P*-values were determined for pairwise comparisons using Student's unpaired *t*-tests. $R^2$ correlation values were calculated in Prism. Bar graphs were created in Prism.

### Data availability statement

No -omics data were generated as a part of this work. Accession numbers for previously generated -omics data are included. Raw data generated from the study are available on reasonable request.

**ORCIDs**
Alice Wang: http://orcid.org/0000-0003-1771-2103
Alexander L. Fogel: http://orcid.org/0000-0001-7835-2127
Michael J. Murphy: http://orcid.org/0000-0001-6494-7250
Gauri Panse: http://orcid.org/0000-0002-5762-3490
Meaghan K. McGeary: http://orcid.org/0000-0002-8505-7158
Jennifer M. McNiff: http://orcid.org/0000-0001-8142-6481
Marcus Bosenberg: http://orcid.org/0000-0003-0166-1612
Matthew D. Vesely: http://orcid.org/0000-0001-9363-945X
Jeffrey M. Cohen: http://orcid.org/0000-0002-7709-0548
Christine J. Ko: http://orcid.org/0000-0003-2270-2524
Brett A. King: http://orcid.org/0000-0002-4576-4616
William Damsky: http://orcid.org/0000-0003-0975-4071

## AUTHOR CONTRIBUTIONS

Conceptualization: WD; Data Curation: AW, WD; Formal Analysis: AW, MJM, MKM, WD; Investigation: AW, WD; Methodology: AW, MJM, MKM, CJK, WD; Resources: GP, JMM, MB, BAK, WD; Software: AW, MKM; Supervision: WD; Visualization: AW, WD; Writing - Original Draft Preparation: AW, ALF, MDV, JMC, CJK, WD; Writing - Review and Editing: AW, CJK, WD

## ACKNOWLEDGMENTS

We would like to thank the staff of Yale Dermatopathology laboratory (New Haven, CT), particularly D. Mekael. WD is supported by a Career Development Award from the Dermatology Foundation. BAK is supported by the Ranjini and Ajay Poddar Fund for Dermatologic Disease Research. This study has been approved by the Yale Institutional Review Board.

## CONFLICT OF INTEREST

MDV's spouse is employed by Regeneron. BAK is an investigator for Concert Pharmaceuticals, Eli Lilly and Company, and Pfizer. BAK is a consultant to and/or has served on advisory boards for Aclaris Therapeutics, Arena Pharmaceuticals, Bristol-Meyers Squibb, Concert Pharmaceuticals, Dermavant Sciences, Eli Lilly and Company, Pfizer, and VielaBio; he is on speaker's bureau for Pfizer, Regeneron, and Sanofi Genzyme. WD has research support from Pfizer and is a consultant for TWi Biotechnology. WD and MB are consultants for Eli Lilly and receive licensing fees from EMD, Sigma, and Millipore in unrelated work. The remaining authors state no conflict of interest.

## REFERENCES

Bai F, Li GG, Liu Q, Niu X, Li R, Ma H. Short-term efficacy and safety of IL-17, IL-12/23, and IL-23 inhibitors brodalumab, secukinumab, ixekizumab, ustekinumab, guselkumab, tildrakizumab, and risankizumab for the treatment of moderate to severe plaque psoriasis: a systematic review and network meta-analysis of randomized controlled trials. J Immunol Res 2019;2019:2546161.

Bankhead P, Loughrey MB, Fernandez JA, Dombrowski Y, McArt DG, Dunne PD, et al. QuPath: open source software for digital pathology image analysis. Sci Rep 2017;7:16878.

Bieber T. Interleukin-13: targeting an underestimated cytokine in atopic dermatitis. Allergy 2020;75:54–62.

Brunner PM, Pavel AB, Khattri S, Leonard A, Malik K, Rose S, et al. Baseline IL-22 expression in patients with atopic dermatitis stratifies tissue responses to fezakinumab. J Allergy Clin Immunol 2019;143:142–54.

Caproni M, Torchia D, Antiga E, Terranova M, Volpi W, del Bianco E, et al. The comparative effects of tacrolimus and hydrocortisone in adult atopic dermatitis: an immunohistochemical study. Br J Dermatol 2007;156:312–9.

Cohen JN, Bowman S, Laszik ZG, North JP. Clinicopathologic overlap of psoriasis, eczema, and psoriasiform dermatoses: a retrospective study of T helper type 2 and 17 subsets, interleukin 36, and β-defensin 2 in spongiotic psoriasiform dermatitis, sebopsoriasis, and tumor necrosis factor α inhibitor-associated dermatitis. J Am Acad Dermatol 2020;82:430–9.

Czarnowicki T, He H, Krueger JG, Guttman-Yassky E. Atopic dermatitis endotypes and implications for targeted therapeutics. J Allergy Clin Immunol 2019;143:1–11.

Doube M, Kłosowski MM, Arganda-Carreras I, Cordelières FP, Dougherty RP, Jackson JS, et al. BoneJ: free and extensible bone image analysis in ImageJ. Bone 2010;47:1076–9.

Garzorz-Stark N, Krause L, Lauffer F, Atenhan A, Thomas J, Stark SP, et al. A novel molecular disease classifier for psoriasis and eczema. Exp Dermatol 2016;25:767–74.

Glickman JW, Han J, Garcet S, Krueger JG, Pavel AB, Guttman-Yassky E. Improving evaluation of drugs in atopic dermatitis by combining clinical and molecular measures. J Allergy Clin Immunol Pract 2020;8:3622–5.e19.

Hanifin JM, Rajka G. Diagnostic features of atopic dermatitis. Acta Derm Venereol Suppl (Stockh) 1980;92:44–7.

Hawkes JE, Yan BY, Chan TC, Krueger JG. Discovery of the IL-23/IL-17 signaling pathway and the treatment of psoriasis. J Immunol 2018;201:1605–13.

He H, Bissonnette R, Wu J, Diaz A, Saint-Cyr Proulx E, Maari C, et al. Tape strips detect distinct immune and barrier profiles in atopic dermatitis and psoriasis. J Allergy Clin Immunol 2021;147:199–212.

Johansen C, Vinter H, Soegaard-Madsen L, Olsen LR, Steiniche T, Iversen L, et al. Preferential inhibition of the mRNA expression of p38 mitogen-activated protein kinase regulated cytokines in psoriatic skin by anti-TNFα therapy. Br J Dermatol 2010;163:1194–204.

Khattri S, Brunner PM, Garcet S, Finney R, Cohen SR, Oliva M, et al. Efficacy and safety of ustekinumab treatment in adults with moderate-to-severe atopic dermatitis. Exp Dermatol 2017;26:28–35.

Kimmel G, Chima M, Kim HJ, Bares J, Yao CJ, Singer G, et al. Brodalumab in the treatment of moderate to severe psoriasis in patients when previous anti-interleukin 17A therapies have failed. J Am Acad Dermatol 2019;81:857–9.

Martini E, Wikén M, Cheuk S, Gallais Sérézal I, Baharom F, Ståhle M, et al. Dynamic changes in resident and infiltrating epidermal dendritic cells in active and resolved psoriasis. J Invest Dermatol 2017;137:865–73.

McGeachy MJ, Cua DJ, Gaffen SL. The IL-17 family of cytokines in health and disease. Immunity 2019;50:892–906.

Miranda E, Roberts J, Novick S, Lapointe JM, Bruijnzeel-Koomen C, Thijs J, et al. Immunohistochemical characterization of the IL-13:IL-4 receptor α axis in the skin of adult patients with moderate to severe atopic dermatitis and healthy controls. J Invest Dermatol 2021;141:440–3.e4.

Miyagaki T, Sugaya M, Suga H, Kamata M, Ohmatsu H, Fujita H, et al. IL-22, but not IL-17, dominant environment in cutaneous T-cell lymphoma. Clin Cancer Res 2011;17:7529–38.

Moy AP, Murali M, Kroshinsky D, Duncan LM, Nazarian RM. Immunologic overlap of helper T-cell Subtypes 17 and 22 in erythrodermic psoriasis and atopic dermatitis. JAMA Dermatol 2015;151:753–60.

Nakajima K, Kataoka S, Sato K, Takaishi M, Yamamoto M, Nakajima H, et al. Stat3 activation in epidermal keratinocytes induces Langerhans cell activation to form an essential circuit for psoriasis via IL-23 production. J Dermatol Sci 2019;93:82–91.

Nazet U, Schröder A, Grässel S, Muschter D, Proff P, Kirschneck C. Housekeeping gene validation for RT-qPCR studies on synovial fibroblasts derived from healthy and osteoarthritic patients with focus on mechanical loading. PLoS One 2019;14:e0225790.

Pachot A, Blond JL, Mougin B, Miossec P. Peptidylpropyl isomerase B (PPIB): a suitable reference gene for mRNA quantification in peripheral whole blood. J Biotechnol 2004;114:121–4.

Quaranta M, Knapp B, Garzorz N, Mattii M, Pullabhatla V, Pennino D, et al. Intraindividual genome expression analysis reveals a specific molecular signature of psoriasis and eczema. Sci Transl Med 2014;6:244ra90.

Reynolds G, Vegh P, Fletcher J, Poyner EFM, Stephenson E, Goh I, et al. Developmental cell programs are co-opted in inflammatory skin disease. Science 2021;371:eaba6500.

Salerno F, Engels S, van den Biggelaar M, van Alphen FPJ, Guislain A, Zhao W, et al. Translational repression of pre-formed cytokine-encoding mRNA prevents chronic activation of memory T cells. Nat Immunol 2018;19:828–37.

Shroff A, Guttman-Yassky E. Successful use of ustekinumab therapy in refractory severe atopic dermatitis. JAAD Case Rep 2014;1:25–6.

Tsoi LC, Rodriguez E, Degenhardt F, Baurecht H, Wehkamp U, Volks N, et al. Atopic dermatitis is an IL-13-dominant disease with greater molecular heterogeneity compared to psoriasis. J Invest Dermatol 2019;139:1480–9.

Ungar B, Pavel AB, Li R, Kimmel G, Nia J, Hashim P, et al. Phase 2 randomized, double-blind study of IL-17 targeting with secukinumab in atopic dermatitis. J Allergy Clin Immunol 2021;147:394–7.

Wang FP, Tang XJ, Wei CQ, Xu LR, Mao H, Luo FM. Dupilumab treatment in moderate-to-severe atopic dermatitis: a systematic review and meta-analysis. J Dermatol Sci 2018;90:190–8.

Yawalkar N, Karlen S, Egli F, Brand CU, Graber HU, Pichler WJ, et al. Down-regulation of IL-12 by topical corticosteroids in chronic atopic dermatitis. J Allergy Clin Immunol 2000;106:941–7.

Zhang L, Yang XQ, Cheng J, Hui RS, Gao TW. Increased Th17 cells are accompanied by FoxP3(+) Treg cell accumulation and correlated with psoriasis disease severity. Clin Immunol 2010;135:108–17.

Zheng Y, Danilenko DM, Valdez P, Kasman I, Eastham-Anderson J, Wu J, et al. Interleukin-22, a T(H)17 cytokine, mediates IL-23-induced dermal inflammation and acanthosis. Nature 2007;445:648–51.